# Parameter Extraction and Optimal Design of Spiral Inductor Using Evolution Strategy and Sensitivity

Jae-Hyeong Ko[1], Koon-Tae Kim[1], Jin-Kyu Byun[2], and Hyeong-Seok Kim[1]

[1]School of Electrical and Electronics Engineering, Chung-Ang University, Seoul 156-756, Korea
[2]School of Electrical Engineering, Soongsil University, Seoul 156-743, Korea

**For precise electromagnetic (EM) field simulation of the spiral inductor, electric conductivity of the inductor substrate is determined by evolution strategy to match the Taiwan Semiconductor Manufacturing Company (TSMC) process. Based on this parameter, patterned ground shield (PGS) of an on-chip spiral inductor is designed using deterministic optimization method. The design parameters are lengths and widths of ground strips and widths of slots. For sensitivity analysis, approximate adjoint variable method is used. Significant increase in $Q$-factor is observed in final design while reduction of inductance is minimal. Spiral inductor with optimized PGS is used in input matching circuit of 2.45-GHz low noise amplifier (LNA), which shows improved noise figure characteristics compared to non-PGS case.**

***Index Terms*—Evolution strategy, optimal design, $Q$-factor, sensitivity analysis, spiral inductor.**

## I. Introduction

ON-CHIP spiral inductors are widely used in a variety of radio frequency integrated circuits (RF ICs). For spiral inductors in silicon-based RF ICs, substrate loss at high frequencies can degrade quality factor ($Q$). Also, noise coupling may appear at gigahertz frequencies. One of the design techniques to overcome this problem is to insert a ground shield to block inductor electric field from entering the silicon. By shielding the substrate from the electric and magnetic fields of the inductor, the induced substrate currents are shunted ground by the shield and improvements in inductor $Q$-factor can be achieved [1]. However, if the solid ground shield is used, it will disturb the inductor's magnetic field. The image current, which is induced in the solid ground shield by the magnetic field of the spiral inductor, flows in a direction opposite to that of the current in the spiral. The resulting negative mutual coupling between the currents reduces the magnetic field, and thus the overall inductance and $Q$-factor [2]. A popular solution to this problem is to use a patterned ground shield (PGS) [1]–[3]. Patterned slots on the PGS cut off the path of induced image current, hence reducing disturbance of inductor magnetic field.

When designing spiral inductor with PGS, many parameters should be considered, including geometric parameters such as widths of ground strips and slots, separation between spiral and ground shield, and lengths of strip. On the other hand, material parameter, i.e., electric conductivity of the substrate, is a crucial factor for accurate analysis and design of the spiral inductor. So far, these design parameters were determined by trial and error in most cases, resulting in high design cost and time.

In this paper, as a setup process of PGS optimal design, electric conductivity of the inductor substrate is first determined by evolution strategy (ES) to match the performance of the Taiwan Semiconductor Manufacturing Company (TSMC) inductor. Then, deterministic optimization method is applied to the optimal shape design of PGS of an on-chip spiral inductor. Design goal is to maximize $Q$-factor while keeping inductance reduction minimal. Sensitivity analysis of the objective function is performed by approximate adjoint variable method.

Manuscript received December 23, 2009; accepted February 21, 2010. Current version published July 21, 2010. Corresponding author: H.-S. Kim (e-mail: kimcaf2@cau.ac.kr).

Color versions of one or more of the figures in this paper are available online at http://ieeexplore.ieee.org.

Digital Object Identifier 10.1109/TMAG.2010.2045114

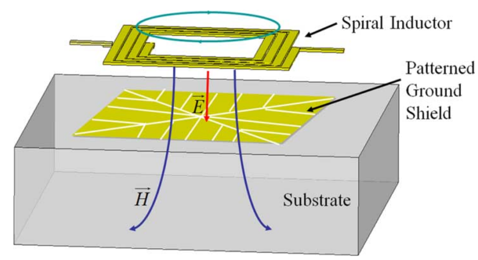


Fig. 1. Spiral inductor with PGS.

## II. Design of Spiral Inductor With PGS

Fig. 1 explains improvement of $Q$-factor of spiral inductor with PGS. Electric field of inductor in substrate direction is blocked by a ground shield and dissipation loss is reduced. Magnetic field disturbance is small because eddy current on ground shield is suppressed by patterned slots.

### A. Parameter Extraction Using Evolution Strategy

If inaccurate electrical parameters of substrates are used, electromagnetic (EM) field simulation and design of inductor will have significant error with respect to the actual measurement data from TSMC. Thus, accurate electric conductivity of the inductor substrate is determined using ES [4], [5] before optimal shape design of PGS is performed. The design goal of ES is to obtain EM simulation results similar to data from TSMC process. Since the main characteristics of inductor are given by inductance $L$ and $Q$-factor, the objective function $F$ is defined as a function of them

$$\text{Minimize } F = \sum_{i=1}^{n} \alpha_i (L_i - L_{oi})^2 + \sum_{i=1}^{n} \beta_i (Q_i - Q_{oi})^2 \quad (1)$$

where $\alpha_i$ and $\beta_i$ are weighting factors for inductance $L_i$ and $Q$-factor $Q_i$ from EM simulation, and $L_{oi}$, $Q_{oi}$ are target values of inductance and $Q$-factor obtained from equivalent circuit analysis of TSMC. The weighting factor for the term with the largest value among the square terms in (1) becomes

0018-9464/$26.00 © 2010 IEEE

Authorized licensed use limited to: JADAVPUR UNIVERSITY. Downloaded on August 10,2010 at 10:56:13 UTC from IEEE Xplore. Restrictions apply.

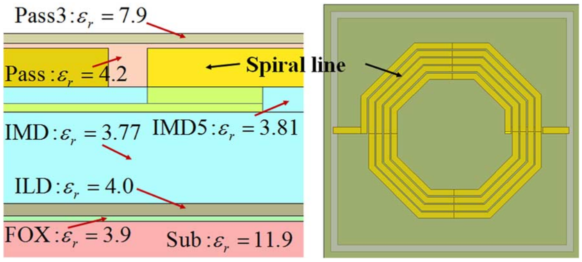


Fig. 2. Spiral inductor of TSMC process which simplifies.

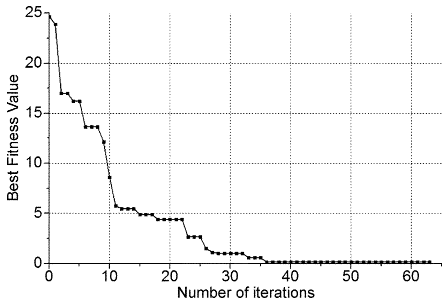


Fig. 3. Convergence of the objective function.

TABLE I
DESIGN PARAMETERS

| Parameter | Unit | Initial values | Optimal values |
|---|---|---|---|
| Pass3 | S/m | 0 | 0.3592 |
| Pass | S/m | 0 | 0.6221 |
| IMD5 | S/m | 0 | 0.0056 |
| IMD | S/m | 0 | 0.0213 |
| ILD | S/m | 0 | 0.0165 |
| FOX | S/m | 0 | 0.0052 |
| Sub | S/m | 10 | 8.6514 |

TABLE II
INDUCTANCE AND $Q$-FACTOR OF SPIRAL INDUCTOR

| Performance | | 1 GHz | 2 GHz | 3 GHz | 4 GHz | 5 GHz |
|---|---|---|---|---|---|---|
| Inductance (nH) | TSMC | 6.425 | 6.731 | 7.235 | 8.017 | 9.234 |
| | Initial | 6.475 | 6.733 | 7.238 | 8.077 | 9.429 |
| | Optimal | 6.444 | 6.691 | 7.159 | 7.918 | 9.078 |
| Q-factor | TSMC | 6.072 | 8.375 | 7.511 | 5.841 | 4.240 |
| | Initial | 6.425 | 9.852 | 10.17 | 8.420 | 6.047 |
| | Optimal | 6.041 | 8.147 | 7.518 | 5.886 | 4.182 |

1, and weighting factors for other terms are set such that each term can be almost equal to the largest value. $n = 10$ is a frequency sampling number. That is, inductance and $Q$-factor are computed from 0.5 to 5 GHz at 0.5-GHz intervals.

For the inductor structure used in simulation with $(1+1)$ ES, the number of the coil turns is 4.5, width of the top metal is 9 $\mu$m, and radius of inner coil is 78 $\mu$m as shown in Fig. 2.

The design parameters are set as electric conductivity of each layer of the substrate, named pass3, pass, IMD5, IMD, ILD, FOX, and Sub (Fig. 2). It is assumed that layers IMD1a$\sim$4b from TSMC process form a single layer (IMD), and IMD5a$\sim$5b form another single layer (IMD5) to simplify the design process and reduce the computation time.

The convergence of the normalized objective function is shown in Fig. 3, where the best solution is at the 63rd iteration. The initial and optimized design values are presented in Tables I and II. Also, inductance and $Q$-factor results are compared in Figs. 4 and 5.

From the results, it can be observed that the performance of the optimized design is analogous to that of TSMC inductor. Tolerance of extracted substrate conductivity is less than 5% in 0.5–5-GHz range.

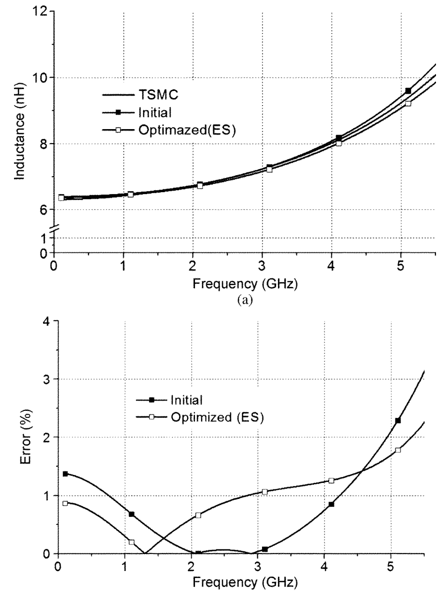


Fig. 4. Comparison of (a) inductance and (b) error before and after ES optimization.

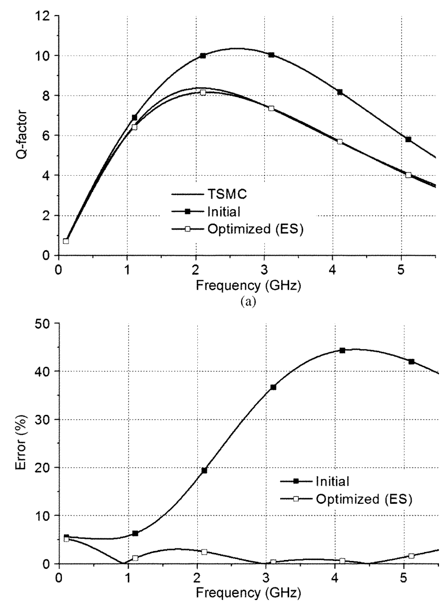


Fig. 5. Comparison of (a) $Q$-factor and (b) error before and after ES optimization.

TABLE IV
INDUCTANCE AND $Q$-FACTOR OF SPIRAL INDUCTOR WITH PGS

| Performance | | 1 GHz | 2 GHz | 3 GHz | 4 GHz | 5 GHz |
|---|---|---|---|---|---|---|
| Inductance (nH) | Non-PGS | 6.444 | 6.691 | 7.159 | 7.918 | 9.078 |
| | Initial | 6.266 | 6.512 | 7.006 | 7.869 | 9.353 |
| | Optimal | 6.429 | 6.674 | 7.170 | 8.035 | 9.515 |
| Q-factor | Non-PGS | 6.041 | 8.147 | 7.518 | 5.886 | 4.182 |
| | Initial | 5.977 | 8.525 | 8.578 | 7.354 | 5.599 |
| | Optimal | 6.121 | 8.748 | 8.848 | 7.620 | 5.826 |

Authorized licensed use limited to: JADAVPUR UNIVERSITY. Downloaded on August 10,2010 at 10:56:13 UTC from IEEE Xplore. Restrictions apply.

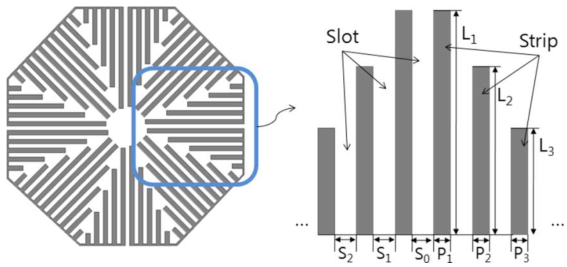


Fig. 6. Initial PGS structure and design variables of PGS.

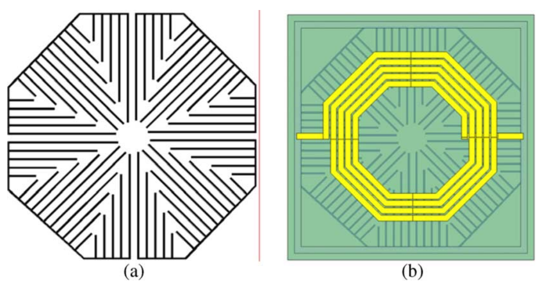


Fig. 7. (a) Optimized PGS structure and (b) spiral inductor with PGS.

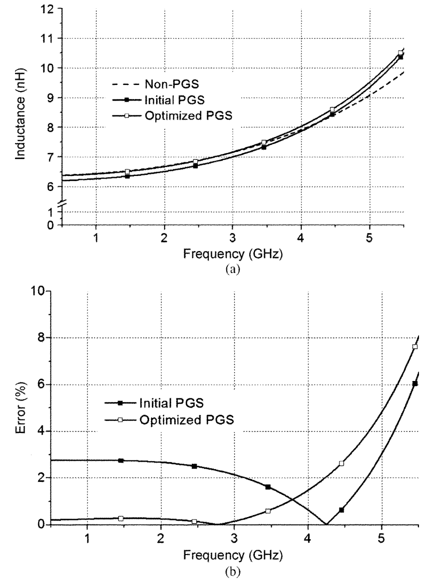


Fig. 8. (a) Inductance profile and (b) difference from the target value before and after optimization.

### *B. PGS Shape Optimization Using Design Sensitivity*

In this section, optimal design of PGS using sensitivity analysis is explained. The design goal is to improve $Q$-factor while maintaining inductance value. The objective function is given in the same form as (1), but $L_{oi}$ and $Q_{oi}$ are target values set by the designer data in this case.

Since the objective function has inductance term and $Q$-factor term, sensitivity is expanded as

$$\frac{dF(L,Q)}{dp} = \frac{\partial F}{\partial L}\frac{\partial L}{\partial p} + \frac{\partial F}{\partial Q}\frac{\partial Q}{\partial p} \tag{2}$$

where $\partial F/\partial L$ and $\partial F/\partial Q$ are explicit terms that are easily obtained. To calculate $\partial L/\partial p$ and $\partial Q/\partial p$ terms, adjoint excitation vectors $\mathbf{G}_L^i$ and $\mathbf{G}_Q^i$ must be derived. They are given by

$$\mathbf{G}_L^i = \mathbf{a}_x\frac{\partial L}{\partial E_x} + \mathbf{a}_y\frac{\partial L}{\partial E_y} + \mathbf{a}_z\frac{\partial L}{\partial E_z} \tag{3}$$

$$\mathbf{G}_Q^i = \mathbf{a}_x\frac{\partial Q}{\partial E_x} + \mathbf{a}_y\frac{\partial Q}{\partial E_y} + \mathbf{a}_z\frac{\partial Q}{\partial E_z}. \tag{4}$$

Since $L$ and $Q$ can be written in terms of field values at the port, these excitation vectors can be derived using algebraic equations.

Finally, the inductance sensitivity term is given by

$$\frac{\partial L}{\partial p_n} = -\iiint_{\Omega} \hat{\mathbf{E}}_L \cdot \frac{\partial R(\mathbf{E})}{\partial p_n} d\Omega \tag{5}$$

where $\hat{\mathbf{E}}_L$ is obtained from the solution of the adjoint equation

$$C_0^2\hat{\mathbf{E}}_L + \alpha_0\hat{\mathbf{E}}_L = \mathbf{G}_L^i \tag{6}$$

and expressions for $C_0^2$ and $\alpha_0$, and $R(\mathbf{E})$ follows approximate adjoint variable formulation [6]. $Q$-factor sensitivity can be calculated using the similar manner.

PGS is designed on the layer of polysilicon with thickness 0.2 $\mu$m and design variables of the PGS structure are show in Fig. 6, where $S_i$ and $P_i$ are the $i$th width of slot and strip, respectively, and $L_i$ is the length of strip.

TABLE III
DESIGN PARAMETERS

| Parameter | | Unit | Initial values | Optimal values |
|---|---|---|---|---|
| Strip | $P_1$-$P_5$ | μm | 6.00 | 2.41 |
| | $L_1$ | μm | 139.44 | 144.29 |
| | $L_2$ | μm | 110.47 | 116.58 |
| | $L_3$ | μm | 81.50 | 88.86 |
| | $L_4$ | μm | 52.53 | 61.15 |
| | $L_5$ | μm | 23.56 | 33.43 |
| Slot | $S_0$ | μm | 6.00 | 9.16 |
| | $S_1$-$S_4$ | μm | 6.00 | 9.07 |

The optimized structure of PGS and design values are presented in Fig. 7 and Table III. The performance of spiral inductor with PGS before and after optimization is compared with that of the spiral inductor with non-PGS in Figs. 8 and 9 and Table IV.

Compared to the non-PGS case, the average improvement of the $Q$-factor of the inductor with optimized PGS is 16.655% below 5 GHz. However, the average reduction of inductance for the same frequency range is only 0.935%.

The comparisons of performance before and after optimization are shown in Figs. 8(b) and 9(b). Compared to the initial design, average $Q$-factor is increased by 3.446%, while difference of inductance from the target value is also improved by 1.233%.

### *C. The 2.45-GHz LNA Design Using Spiral Inductor With PGS*

To show the effectiveness of the inductor with optimized PGS, the single band low noise amplifier (LNA) operating at 2.45 GHz is designed based on TSMC process. High $Q$ of the input circuit can reduce noise factor of LNA [7], [8]. Thus, inductor with optimized PGS is used to improve $Q$-factor of the input circuit. Fig. 10 shows schematic of LNA, which is designed using power-constrained simultaneous noise and input matching (PCSNIM) technique [7]. Positive supply voltage (VDD) and gate voltage (VGS) are 1.8 V and 1.4 V, and input inductor (Lg) is 6.93 nH. The inductance and $Q$-factor of spiral

Authorized licensed use limited to: JADAVPUR UNIVERSITY. Downloaded on August 10,2010 at 10:56:13 UTC from IEEE Xplore. Restrictions apply.

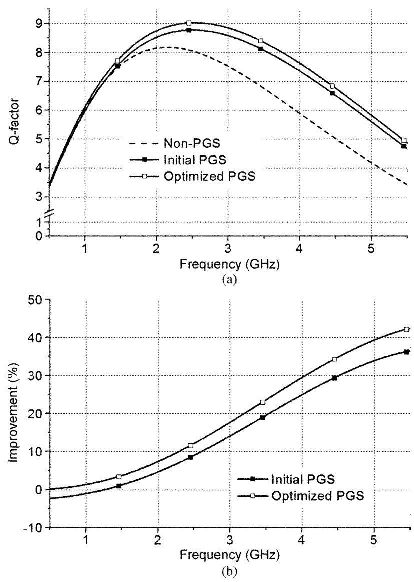


Fig. 9. Comparison of (a) $Q$-factor and (b) improvement ratio before and after optimization.

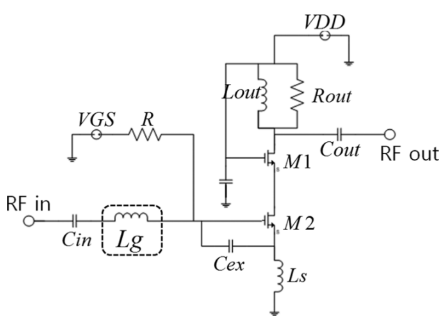


Fig. 10. Schematic of LNA.

TABLE V
INDUCTANCE AND $Q$-FACTOR OF SPIRAL INDUCTOR AT 2.45 GHz

| Type | Inductance (nH) | Q-factor |
|---|---|---|
| Non-PGS | 6.871 | 8.082 |
| Optimal PGS | 6.861 | 9.020 |

inductors with no PGS and optimized PGS at LNA frequency of 2.45 GHz are presented in Table V. It can be seen both have inductance value very close to the input inductor of LNA.

Each inductor in Table V is substituted for Lg of LNA, and LNA simulation is performed. Fig. 11 shows $S$-parameter and noise figure (NF) of LNA with optimized PGS and non-PGS.

In order to obtain the same gain as 17.714 dB, VGS of LNA with optimized PGS is adjusted to 1.319 V. Table VI shows $S$-parameter and NF at 2.45 GHz when gains of LNA with non-PGS and optimized PGS are identical. LNA with optimized PGS reduces NF by 4.59% compared to that with non-PGS. It is believed that high $Q$-factor of the input inductor is responsible for this improvement of LNA NF.

## III. CONCLUSION

In this paper, $Q$-factor of the on-chip spiral inductor was improved by optimizing PGS structure while keeping inductance reduction minimal. Complex electrical permittivity of the each layer of spiral inductor was extracted by ES. Using discrete sensitivity analysis, various geometrical parameters of the PGS structure were optimized. Spiral inductor with optimized PGS is used in the LNA design, which shows improved noise figure characteristics compared to non-PGS case.

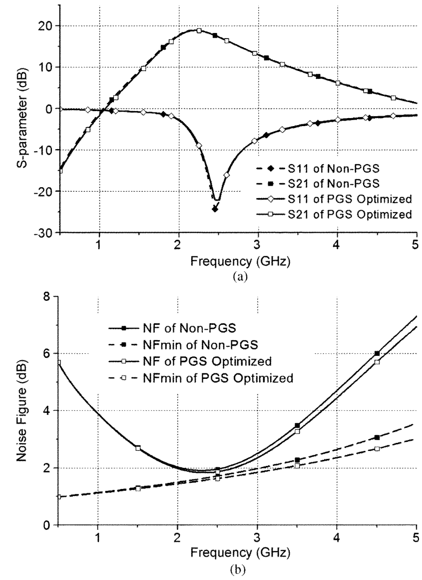


Fig. 11. Comparison of (a) $S$-parameter and (b) noise figure between LNA using non-PGS inductor and inductor with optimized PGS.

TABLE VI
GAIN AND NOISE FIGURE AT 2.45-GHz LNA

| Type | Unit | S11 | NF | NFmin |
|---|---|---|---|---|
| Non-PGS | dB | -24.343 | 1.933 | 1.688 |
| Optimal PGS | dB | -22.065 | 1.844 | 1.605 |

## ACKNOWLEDGMENT

This work was supported by the Basic Science Research Program through National Research Foundation of Korea (NRF) funded by the Ministry of Education, Science and Technology (2009-0076366).

## REFERENCES

[1] R. Svitek, A. S. Klein, M. Clifford, and S. Raman, "Development of scalable models for patterned-ground-shield inductors in SiGe BiCMOS technology," in *Proc. Silicon Monolithic Integrated Circuits RF Syst.*, 2004, Sep. 2004, pp. 211–214.

[2] C. P. Yue and S. S. Wong, "On-chip spiral inductors with patterned ground shields for Si-based RF IC's," *IEEE J. Solid-State Circuits*, vol. 33, no. 5, pp. 743–752, May 1998.

[3] J. Shi, W. Y. Yin, K. Kang, J. F. Mao, and L. W. Li, "Frequency-thermal characterization of on-chip transformers with patterned ground shields," *IEEE Trans. Microw. Theory Tech.*, vol. 55, no. 1, pp. 1–12, Jan. 2007.

[4] S. D. Muller, N. N. Schraudolph, and P. D. Koumoutsakos, "Step size adaptation in evolution strategies using reinforcement learning," in *Proc. Congr. Evol. Comput.*, May 2002, vol. 1, pp. 151–156.

[5] T. Back, *Evolutionary Algorithms in Theory and Practice*. Oxford, U.K.: Oxford Univ. Press, 1996.

[6] N. K. Nikolova, X. Zhu, Y. Song, A. Hasib, and M. H. Bakr, " $S$-parameter sensitivities for electromagnetic optimization based on volume field solutions," *IEEE Trans. Microw. Theory Tech.*, vol. 57, no. 6, pp. 1526–1538, Jun. 2009.

[7] P. Andreani, "Noise optimization of an inductively degenerated CMOS low noise amplifier," *IEEE Trans. Circuits Syst.*, vol. 48, pp. 835–841, Sep. 2001.

[8] D. K. Shaeffer and T. H. Lee, "A 1.5-V, 1.5-GHz CMOS low noise amplifier," *IEEE J. Solid-State Circuits*, vol. 32, no. 5, pp. 745–759, May 1997.

Authorized licensed use limited to: JADAVPUR UNIVERSITY. Downloaded on August 10,2010 at 10:56:13 UTC from IEEE Xplore. Restrictions apply.